Quantitative Fundus Autofluorescence in Pseudoxanthoma Elasticum

Martin Gliem,[1,2] Philipp L. Müller,[1,2] Johannes Birtel,[1,2] Myra B. McGuinness,[3] Robert P. Finger,[1] Philipp Herrmann,[1,2] Doris Hendig,[4] Frank G. Holz,[1,2] and Peter Charbel Issa[1,2,5]

[1]Department of Ophthalmology, University of Bonn, Bonn, Germany
[2]Center for Rare Diseases Bonn (ZSEB), University Hospital of Bonn, Bonn, Germany
[3]Centre for Eye Research Australia, University of Melbourne, Melbourne, Australia
[4]Institute for Laboratory and Transfusion Medicine, Heart and Diabetes Center North Rhine-Westphalia, University Hospital of the Ruhr University of Bochum, Bad Oeynhausen, Germany
[5]Oxford Eye Hospital, Oxford University Hospitals NHS Foundation Trust and the Nuffield Laboratory of Ophthalmology, Department of Clinical Neurosciences, University of Oxford, Oxford, United Kingdom

Correspondence: Peter Charbel Issa, Oxford Eye Hospital, John Radcliffe Hospital, Headley Way, Oxford OX3 9DU, UK;
study-enquiry@outlook.com.

Submitted: April 7, 2017
Accepted: October 29, 2017

Citation: Gliem M, Müller PL, Birtel J, et al. Quantitative fundus autofluorescence in pseudoxanthoma elasticum. *Invest Ophthalmol Vis Sci*. 2017;58:6159–6165. DOI:10.1167/iovs.17-22007

Purpose. To quantify lipofuscin-associated fundus autofluorescence in patients with pseudoxanthoma elasticum (PXE), a model disease for Bruch's membrane pathology.

Methods. In this prospective, monocenter, cross-sectional case-control study, 49 patients with PXE (mean age: 46 years, range 18–62) underwent quantitative fundus autofluorescence (qAF) imaging with a modified scanning laser ophthalmoscope containing an internal fluorescent reference for normalization of images. The mean qAF values of a circular ring centered on the fovea (qAF_8) were measured and compared to 108 healthy controls (mean age 40 years, range 18–64).

Results. Overall, patients with PXE showed lower qAF_8 values compared to controls (difference from controls −23%, 95% confidence interval [CI] −29% to −16%, $P < 0.001$). The reduction was most pronounced in patients older than 40 years (−30%, 95% CI −36% to −23%, $P < 0.001$) and was negatively correlated with the extent of Bruch's membrane calcification ($r = -0.49$, 95% CI: −0.67 to −0.22). The topographic distribution revealed a greater reduction of qAF values toward the optic disc than temporally compared to controls ($P < 0.001$). The phenotype of patients with reduced qAF values was characterized by pattern-dystrophy-like changes (71%; 10 of 14), reticular pseudodrusen (71%; 10 of 14) and limited areas of atrophy (29%, 4 of 14).

Conclusions. Reduced qAF_8 values are a characteristic finding in patients with PXE, indicating that Bruch's membrane disease may result in a modification of the accumulation, distribution, or composition (or a combination thereof) of lipofuscin in retinal pigment epithelial cells.

Keywords: pseudoxanthoma elasticum, Bruch's membrane, autofluorescence, quantitative fundus autofluorescence, retinal pigment epithelium

Quantitative fundus autofluorescence (qAF) may be used as a surrogate marker for lipofuscin accumulation in the RPE.[1] Lipofuscin has been associated with toxic effects on the RPE[2,3] and is therefore considered as an important pathogenic factor in various retinal diseases, including AMD.[4] Using qAF imaging, we recently showed that patients with early and intermediate AMD have normal or low qAF levels when compared to age-related controls.[5] The reason for this rather unexpected finding has as yet remained a matter of hypothesis and speculations.

Among other possible explanations, dysfunction of the choroid-Bruch's membrane–RPE complex was discussed, which could possibly lead to slowing of the visual cycle.[5] Reduced turnaround of vitamin A derivatives would hence result in reduced lipofuscin accumulation and lower qAF measures. An important factor in this context could be pathology of Bruch's membrane, which is known to occur in AMD.[6] A diseased Bruch's membrane could then lead to an increased resistance for vitamin A molecules to enter the visual cycle from the choroid. Furthermore, an altered metabolism of RPE cells overlying a pathologic Bruch's membrane could interfere with normal visual cycle dynamics.

Pseudoxanthoma elasticum (PXE; OMIM# 264800) may be used as a model disease to study the effects of a primary ocular pathology in Bruch's membrane. The ocular phenotype of PXE is characterized by an early onset calcification of Bruch's membrane, which starts posteriorly close to the optic disc and spreads toward the periphery over time. The transition zone between the centrally calcified and peripherally noncalcified Bruch's membrane forms a speckled area, the so-called "peau d'orange," which is usually most prominent temporally.[7,8] Secondary to the calcification of Bruch's membrane, other PXE-related fundus changes may develop, including angioid streaks; reticular pseudodrusen (RPD); choroidal neovascularization (CNV); and areas of atrophy.[8–10] Overall, the ocular phenotype in patients with PXE shows similarities with AMD, suggesting

common pathogenic pathways at the level of Bruch's membrane.

The aim of this study was to further explore the hypothesis that Bruch's membrane changes could result in reduced lipofuscin-related qAF measures. For this purpose, we investigated the impact of a diseased Bruch's membrane on lipofuscin-levels within the RPE using qAF imaging in patients with PXE.

Materials And Methods

This prospective cross-sectional case-control study was conducted in adherence to the tenets of the Declaration of Helsinki. Institutional review board approval (Ethikkommission, Medizinische Fakultät, Rheinische Friedrich-Wilhelms-Universität Bonn) and patient consent were obtained. Patients were recruited from a dedicated clinic for rare retinal degenerations at the Department of Ophthalmology, University of Bonn, which serves as the German national referral center for PXE.

Inclusion criteria were the diagnosis of PXE based on clinical findings typical for PXE including peau d'orange, angioid streaks, and peripheral comet lesions as well as genetic testing as described previously[11,12] and/or histopathologic findings in skin biopsies.[13]

Exclusion criteria were aged <18 and >65 years, any pathology affecting the ocular media such as corneal opacities, cataract unusual for age, pseudophakia, vitreous opacities, pupil diameter <7 mm, CNV-related changes (e.g., fibrosis, intra-/subretinal fluid) within the area of qAF measurement, unstable fixation, refractive error ±6 diopters (spherical equivalent), atrophy >50% within the area of measurement or any other pathology of the macular region not related to PXE.

Image Recordings and Analysis

Prior to imaging, pupils were dilated by instillation of 0.5% tropicamide and 2.5% phenylephrine. All subjects underwent a standardized imaging protocol consisting of fundus photography (Visucam; Carl Zeiss Meditec, Jena, Germany); spectral-domain optical coherence tomography (SD-OCT); near-infrared (NIR) reflectance; and fundus autofluorescence (AF) imaging with a confocal scanning laser ophthalmoscope (486-nm excitation, Spectralis HRA+OCT; Heidelberg Engineering, Heidelberg, Germany).

QAF imaging was performed as described previously according to the method developed by Delori et al.[1,14] Briefly, an OCT device (Spectralis HRA; Heidelberg Engineering) was equipped with an internal fluorescent reference to account for fluctuations in laser power and differences in detector sensitivity. After switching to the qAF mode (486-nm excitation and 500–680 nm detection) focus and alignment were adjusted to obtain a maximum and uniform signal. The visual pigment was bleached for at least 20 to 30 seconds. A series of 12 successive images was recorded using the customized software developed by Heidelberg Engineering (30° field of view and 768 × 768 pixels). The quality of the acquired images was evaluated after recording. Images were excluded in cases of insufficient quality (e.g., inhomogeneous illumination, sectorial opacities such as those produced by eyelashes or floaters, or unstable fixation). A minimum of nine remaining images were required for further analysis. Images were averaged and saved without normalization. The right eye was used for analysis. In cases of poor image quality, anatomic abnormalities or progressed fundus alterations the left eye was used instead ($n = 13$).

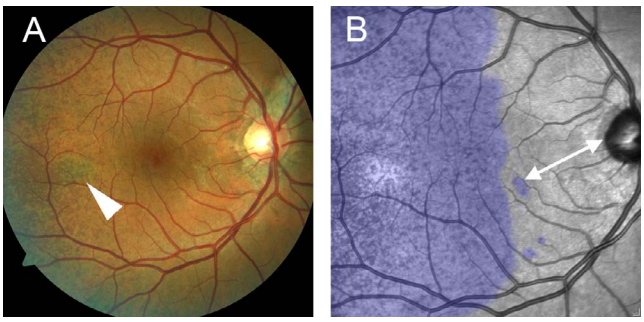

Figure 1. Visualization of Bruch's membrane calcification in PXE. (**A**) Fundus color and (**B**) near-infrared (NIR) reflectance images of a 32-year-old representative patient with PXE. Peau d'orange highlights the circular transformation zone between the centrally calcified and peripherally noncalcified Bruch's membrane, which is best visible at the temporal fundus as brownish speckles that contrast with central abnormal whitish fundus reflex ([**A**], *arrowhead*). Its eccentricity can therefore be regarded as a measure for the eccentricity of Bruch's membrane calcification (EBC). The visualization is enhanced on NIR reflectance images with darker spots within the centrally enhanced reflectivity, allowing improved detection and measurement of the EBC (area of peau d'orange visualized in blue, arrow marks measured EBC).

For image analysis, data was exported from the ophthalmic imaging software (Heidelberg Eye Explorer; Heidelberg Engineering) to a customized image analysis program written in IGOR (see Acknowledgements). The mean gray values of the reference and a circular region with eight subsegments and an eccentricity of approximately 7° to 9° centered on the fovea were measured. Retinal vessels, areas of atrophy, or reduced autofluorescence due to angioid streaks[15] were excluded from analysis by automated histogram analysis. The gray values were exported to a spreadsheet analysis program (Excel; Microsoft, Redmond, WA, USA). QAF values were calculated based on the formula described by Delori et al.,[1] accounting for the gray value of the reference and the eight segments; the zero-level of the laser; the magnification; the age-adjusted lens opacity (based on normative data); and a device-specific calibration factor. The overall qAF value was computed as the mean of the qAF values of the eight segments (qAF_8). QAF_8 values were compared to 108 healthy controls of Caucasian ethnicity (age range, 18–64 years) without any eye disease. More central and peripheral segments were not analyzed due to the decreasing reliability of measurements (e.g., macular pigment within central segments and decreasing field uniformity and repeatability within peripheral segments).[1]

Color-coded qAF maps were computed based on pixel-wise transformation of qAF values into colors using a custom-made extension of the ophthalmic imaging software (Heidelberg Engineering).

To assess the extent of Bruch's membrane calcification, the temporal eccentricity of peau d'orange (or "eccentricity of the leading edge of Bruch's membrane calcification": EBC) was used, although its formal validation as a surrogate marker for disease progression is pending. The EBC was shown to be associated to other PXE-related findings, such as angioid streaks that only occur within calcified areas,[7] and reticular pseudodrusen (RPD).[7,9] The EBC was measured based on 30° NIR reflectance images (due to the higher sensitivity compared with fundus color images to detect peau d'orange[15]) using the integrated measurement tool of the ophthalmic imaging software (Heidelberg Engineering). Measurement was performed from the temporal edge of the optic disc to the most central border of peau d'orange in the temporal (mid-) periphery (Fig. 1).[9] If peau d'orange was not

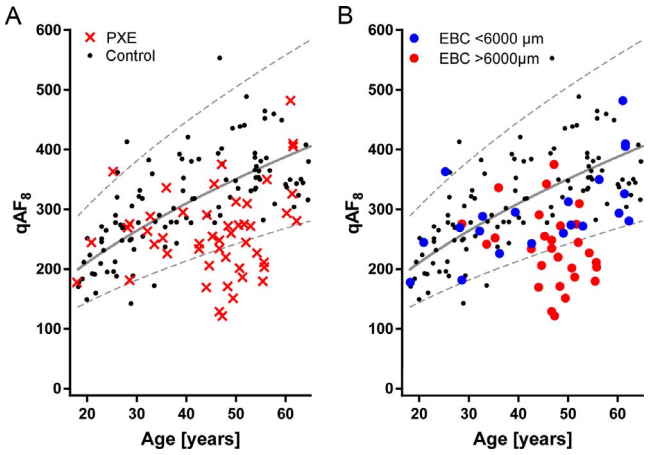

FIGURE 2. Quantitative fundus autofluorescence in PXE. (**A**) qAF_8 values of patients with PXE (*red crosses*) compared to healthy controls (*black dots*). (**B**) The graph differentiates eyes with limited (*blue dots*) from those with widespread (*red dots*) Bruch's membrane calcification. *Continuous gray line*: regression curve of controls. *Dashed curve*: 95% PI of controls. *EBC*: eccentricity of the leading edge of Bruch's membrane calcification.

visible on 30° images in progressed cases, 55° images were used instead, which may affect accuracy ($n = 8$).

Statistical Analysis

Data were collected and illustrated using spreadsheet (Microsoft Corp.) and graphing software (GraphPad Prism version 6; GraphPad Software, Inc., La Jolla, CA, USA). Statistical analysis was performed using statistical software (SPSS version 20.0; IBM Corp., Armonk, NY, USA; and Stata/IC version 13.1; College Station, TX, USA). Prediction intervals (PI) were calculated assuming a linear relationship between the log of age and the log of qAF_8 units for all control subjects. Linear regression of the log of qAF_8 was used to compare patients to controls adjusting for the log of age. Effect modification by segment (nasal versus temporal) was investigated in a separate model which included interactions between segment and PXE status and robust standard errors to account for intraperson correlation. For further analysis, the standardized residuals from this model were calculated to form age-standardized scores (z-score).[16] The extent of Bruch's membrane calcification was compared between groups by one factorial analysis of variance followed by Tukey's test for the pairwise comparison of groups. The correlation between Bruch's membrane calcification and qAF was assessed by calculating the Pearson's correlation coefficient. The topographic distribution of qAF values along the qAF_8 circle was compared using 2-tailed Student's t-test after data distribution was confirmed to be Gaussian. Categorical variables were assessed using Fisher's exact test.

RESULTS

The study included 49 individuals with PXE (36 female, 13 male) with a mean age of 46 years (range, 18–62 years) and 108 controls (72 female, 36 male) without any eye disease (mean age 40, range: 18–64 years). Molecular genetic testing revealed two disease-causing *ABCC6*-mutations in 34 patients, and one disease-causing mutation in seven patients. In another seven patients, PXE was confirmed by positive histopathologic findings in skin biopsies. The diagnosis was based on clinical findings alone in 1 patient.

Quantitative Autofluorescence

Measurement of qAF_8 revealed values within the age-related 95% prediction interval (PI) of controls in 34 patients (69%). QAF_8 was below the 95% PI in 14 (29%) and above in one (2%) patient (Fig. 2A). After adjusting for age statistical analysis revealed overall reduced qAF_8 values in PXE patients compared to controls (difference from controls −23%, 95% CI −29% to −16%, $P < 0.001$).

In younger patients below 40 years of age ($n = 13$), qAF_8 was within the 95% PI in 12 (92%) patients and slightly above in one patient (Fig. 2A). Accordingly, statistical analysis showed no significant difference compared to controls (difference from controls −3%, 95% CI −14 to −11%, $P = 0.728$). In patients 40 years and older ($n = 36$), 14 (39%) had qAF_8 values below the 95% PI and statistical analysis showed an overall significantly lower qAF_8 level for cases compared to controls (difference from controls −30%, 95% CI −36% to −23%, $P < 0.001$).

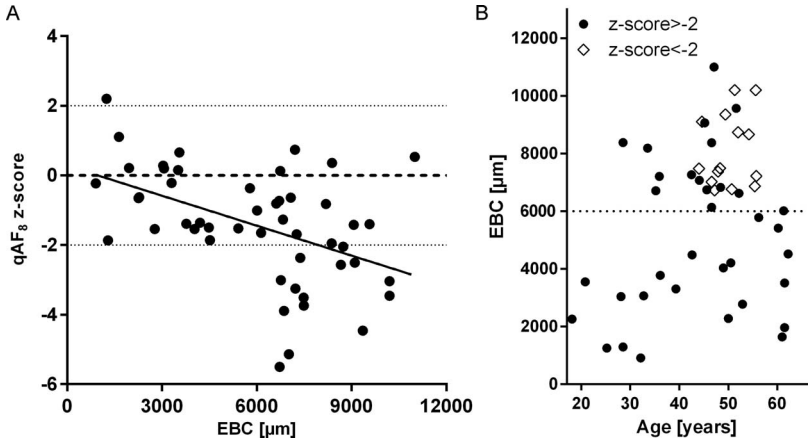

FIGURE 3. Correlation of the extent of Bruch's membrane calcification with qAF_8 z-scores and age in PXE. The qAF_8 z-score represents the number of SDs individual qAF_8 values deviate from the age-related mean of controls. The z-scores (*black dots*) were negatively correlated with the extent of Bruch's membrane calcification, measured as EBC (eccentricity of the leading edge of Bruch's membrane calcification [**A**]). *Dashed line*: z-score 0, representing the mean of controls. *Dotted line*: ±2 SDs. (**B**) EBC increased with age but showed substantial variability. Patients with z-scores < −2 (representing patients with qAF values below 2 SDs of controls) all had an EBC >6000 µm (represented by *dotted line*).

A possible biomarker for the extent of PXE-related ocular effects is the eccentricity of the leading edge of Bruch's membrane calcification (EBC, see methods),[7,9] For a better visualization of a possible association between EBC and qAF_8 values, eyes were differentiated into those with limited (blue dots) and those with more widespread (red dots) Bruch's membrane calcification, arbitrarily defined as an EBC below or above 6000 µm (approximately 20°, meaning peau d'orange only visible at the temporal border of 30° NIR reflectance images, Fig. 2B). Based on this grouping widespread calcification was present in all eyes (14 of 14) with qAF_8 values below the 95% PI (mean EBC ± SD; 8085 ± 1212 µm), but in only 40% (14 of 35) of eyes with normal qAF_8 levels (5090 ± 2613 µm; $P < 0.001$). The graph also illustrates older age not necessarily being associated with more extensive peau d'orange and/or low qAF due to the variable disease manifestation in PXE.

To correlate qAF_8 values with EBC, qAF_8 *z*-scores were calculated. The *z*-score is independent from age, as it represents the number of SDs of a qAF_8 value from the mean of age-related controls. QAF_8 *z*-scores were negatively correlated with EBC ($r = -0.47$, 95% CI −0.67; −0.22; $P < 0.001$, Fig. 3A). Plotting EBC over age illustrated that calcification increased with aging, although with substantial variability. Patients with a *z*-score 2 SDs below average are usually those at older age with more progressed calcification (Fig. 3B).

The overall topographic distribution of qAF values was comparable between controls and PXE patients with highest values in the superotemporal/temporal and lowest values in the nasal sector. However, reduced qAF_8 levels in patients compared to controls were more pronounced close to the optic disc compared with eccentric (temporal) areas indicating a topographic association with the calcification of Bruch's membrane. This is in line with an earlier and more extensive calcification of Bruch's membrane in the papillomacular region, from where it spreads centrifugally toward the periphery. To further illustrate this finding, individual qAF levels from the temporal and nasal segments were plotted for patients and controls (Figs. 4D, 4E). Quantitative analysis revealed a greater difference of qAF values between patients and controls in the nasal segment (24% difference from controls, 95 CI: 21%–27%) than in the temporal segment (9% difference from controls, 95% CI: −7% to −10%). This difference in effect size between segments was significant (interaction term: 0.187 log qAF units, 95% CI: 0.142–0.232, $P < 0.001$, Figs. 4D, 4E).

Eyes of PXE patients with reduced qAF values showed characteristic fundus changes (Figs. 5D–F), including eccentric EBC; pattern dystrophy-like changes (71%, 10 of 14); reticular pseudodrusen (71%, 10 of 14); and limited atrophy (29%, 4 of 14). Such fundus features were significantly less frequent in patients with normal qAF values (pattern dystrophy-like changes: 11 of 35, 31%; $P = 0.023$; reticular pseudodrusen: 9 of 35, 26%; $P = 0.008$; atrophy: 2 of 35, 6%; $P = 0.048$, Figs. 5A–C). Notably, eyes with advanced fundus alterations such as widespread atrophy or fibrosis were not included in the study.

Discussion

This study indicates that a diseased Bruch's membrane in patients with PXE is associated with reduced qAF measures. When corrected for age, there was an inverse relationship between qAF levels and more advanced ocular manifestations of PXE, which include the extent of Bruch's membrane calcification, pattern dystrophy-like changes, reticular pseudodrusen, and atrophy. This finding across the entire cohort is supported by the topographically resolved analysis within eyes

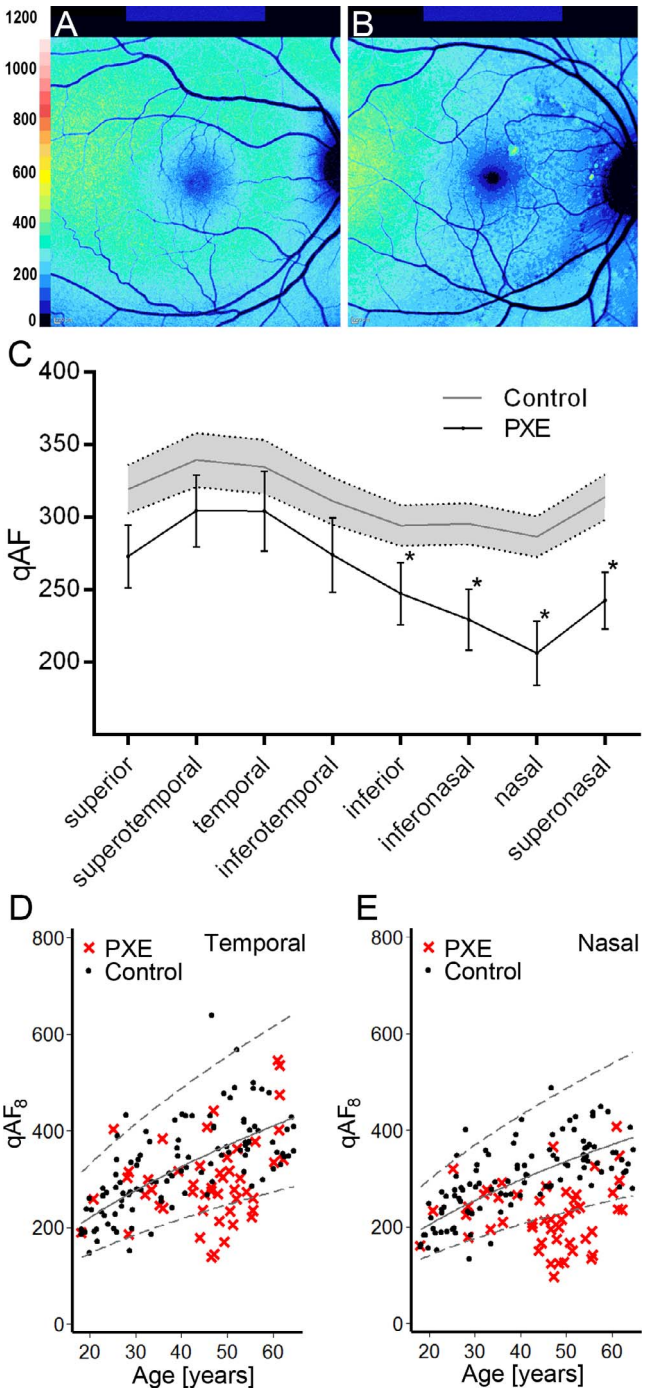

Figure 4. Topographic distribution of quantitative fundus AF in PXE. The images represent color-coded qAF maps showing a pronounced reduction of qAF values nasally in a representative patient with PXE (**B**) compared to an age-matched healthy control ([**A**], both aged 42 years). The graph in (**C**) represents the topographic distribution of mean qAF values of patients with PXE along the qAF_8-circle compared to controls. QAF values were overall reduced in PXE patients with a most pronounced reduction of qAF values close to the optic disc. The *gray area* and the *error bars* represent the 95% CI of controls and PXE patients, respectively. *Indicates differences between controls and PXE patients with $P < 0.001$. The graphs in (**D**, **E**) visualize the qAF_8 values of the temporal (**D**) and nasal segment (**E**) of patients with PXE (*red crosses*) compared to healthy controls (*black dots*). Patients with PXE showed a greater reduction of qAF values in the nasal segment than in the temporal segment compared to controls. *Continuous gray line*: regression curve of controls. *Dashed curve*: 95% prediction interval of controls.

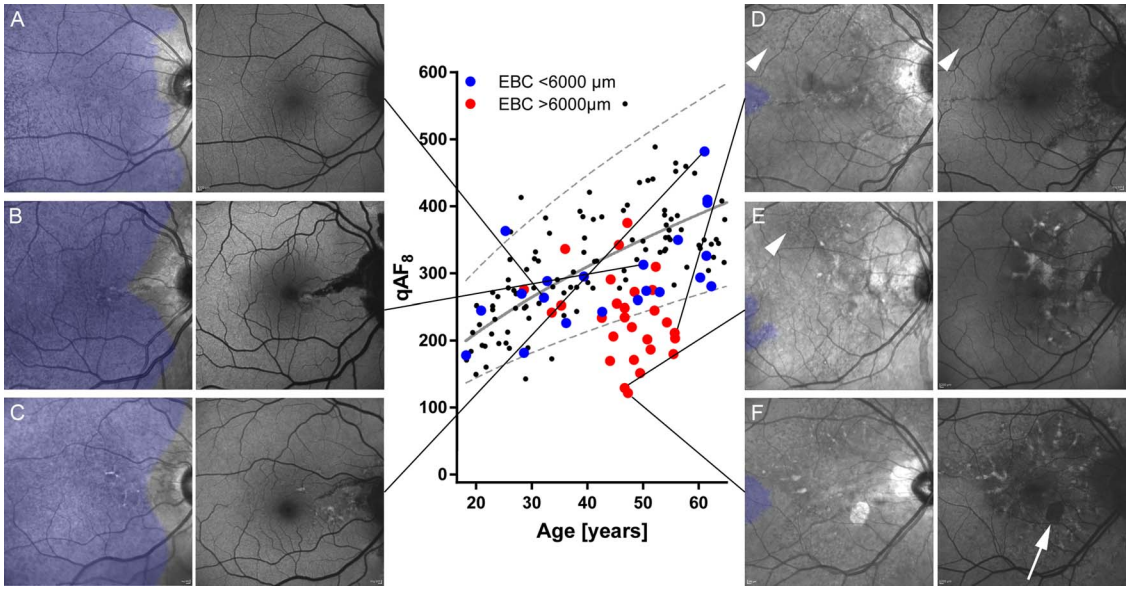

Figure 5. Association of phenotype and quantitative fundus AF in PXE. The graph represents the qAF values and the extent of temporal peau d'orange as shown in Figure 2. The images show representative examples of certain subgroups using NIR reflectance (*left*) and fundus AF images (*right*). Note that the gray levels of the AF images do not represent AF signal intensity (qAF), which was calculated based on comparison with the gray level of a simultaneously recorded AF reference. Younger patients typically presented only mild changes like angioid streaks and relatively central peau d'orange (**A**). Midaged patients with normal qAF values typically showed mild fundus changes and less progressed peau d'orange (**B**). Older patients, again with normal qAF values, frequently had only mild fundus changes like subtle pattern dystrophy-like changes and relatively central peau d'orange (**C**). Patients with reduced qAF values typically showed reticular pseudodrusen ([**D**], *arrowhead*); central pattern dystrophy-like changes (**E**, **F**); and areas of atrophy ([**F**], *arrow*), as well as progressed peau d'orange (graph, peau d'orange marked in *blue* on NIR reflectance images).

individually showing relatively lower values nasally where PXE-associated Bruch's membrane calcification is considered to be most severe.[7] Older patients with relatively normal qAF levels seemed to represent patients at the milder end of the highly variable ocular spectrum of manifestations in PXE. Thus, although the investigated cohort is relatively small, normal age-adjusted qAF levels might represent a favorable (prognostic) parameter in patients with Bruch's membrane disease.

Reduced qAF-levels in patients with PXE may suggest reduced lipofuscin content in the RPE. Although pathophysiologic considerations remain speculative, this finding is in agreement with a hypothesized slowing of the visual cycle as a result of a diseased Bruch's membrane.[5] Possible explanations include an increased barrier function of Bruch's membrane as well as concomitant alterations of the inner choroid resulting in reduced availability of vitamin A and impaired RPE metabolism. Consistently, patients with PXE (own unpublished observations) as well as patients with Sorsby fundus dystrophy[17] and late-onset retinal degeneration (LORD)[18], which demonstrate pathophysiologic overlap at the level of the Bruch's membrane-RPE interface, typically show prolonged dark adaption consistent with a slowdown of the visual cycle. To further confirm this hypothesis investigation of qAF levels in patients with Sorsby fundus dystrophy or LORD would be meaningful.

A diseased Bruch's membrane may also lead to RPE atrophy.[10,19] This process might not only result in areas of complete RPE loss, but also in reduced cell density of the remaining RPE layer. The latter situation would offer an alternative explanation for low qAF levels even if the lipofuscin content in individual cells would be similar to normal controls.

In a previous interpretation of similar findings in AMD patients[5], additional explanations (or a combination thereof) for lower qAF measurements included different packing, density or distribution of lipofuscin within RPE cells, altered composition of fluorophores or blockage by intracellular (e.g., melanin) or extracellular structures (e.g., subretinal drusenoid deposits). Further studies focusing on the exact composition and distribution of fluorophores are therefore needed.

Moreover, measurements could also be affected by PXE-related pathology of the ocular fundus. To overcome this, patients with advanced CNV, fibrosis, or atrophy within the area of measurement were excluded herein. In addition, smaller areas of atrophy (<50% of the area) or pronounced angioid streaks were excluded by histogram analysis.[20] Milder changes such as subtle angioid streaks, pattern dystrophy-like changes or reticular pseudodrusen could have impacted qAF measurements,[5] although these would unlikely explain the effect size observed in older PXE patients.

The observations of this study may be of wider interest when PXE is considered as a model disease for Bruch's membrane pathology. For instance, AMD has a complex pathophysiology and the reasons for the recently reported decreased qAF remain to be determined. Among other contributing pathways,[21,22] it is thought that changes of Bruch's membrane play an important role in the pathogenesis of AMD, including thickening and calcification,[23,24] deposition of advanced glycation end products,[25] and lipid accumulation.[26,27] Furthermore, AMD and PXE-related ocular alterations share phenotypic similarities consistent with common pathogenic pathways at the level of Bruch's membrane. As the current study suggests an association between Bruch's membrane disease and lipofuscin-related qAF levels, one could speculate that Bruch's membrane pathology might at least partially contribute to the reduced qAF levels observed in patients with AMD. Interestingly, prolonged dark adaption has also been reported in patients with AMD.[28,29] Therefore, impairment of visual cycle dynamics could also be a coherent explanation for reduced lipofuscin accumulation in AMD, although further studies are needed to confirm this hypothesis.

In conclusion, this study provides evidence that pathologic changes of Bruch's membrane may be associated with reduced qAF, indicating reduced lipofuscin levels within the RPE. These findings do not only expand the pathophysiologic understanding of PXE, but also of multifactorial diseases with pathologic changes of Bruch's membrane including AMD.

Acknowledgments

The authors thank François Delori, PhD (Schepens Eye Research Institute and Department of Ophthalmology, Harvard Medical School, Boston, MA, USA), who provided the IGOR software that was developed in conjunction with the Department of Ophthalmology at Columbia University (New York, NY, USA). He was not financially compensated for this contribution.

Supported by the National Institute for Health Research (NIHR) Oxford Biomedical Research Centre (BRC); ProRetina Deutschland, Aachen, Germany; the BONFOR research program of the University of Bonn, Bonn, Germany (O-137.0018); and the National Health and Medical Research Council (NHMRC) Centre for Clinical Research Excellence Grant #529923, Canberra, Australia. The Department of Ophthalmology, University of Bonn, receives research support from Heidelberg Engineering. The Centre for Eye Research Australia receives Operational Infrastructure Support from the Victorian Government. The authors alone are responsible for the content and writing of the paper. The views expressed are those of the authors and not necessarily those of the NHS, the NIHR or the Department of Health.

Disclosure: **M. Gliem**, None; **P.L. Müller**, None; **J. Birtel**, None; **M.B. McGuinness**, None; **R.P. Finger**, None; **P. Herrmann**, None; **D. Hendig**, None; **F.G. Holz**, Heidelberg Engineering (C), Zeiss (C); **P. Charbel Issa**, None

References

1. Delori F, Greenberg JP, Woods RL, et al. Quantitative measurements of autofluorescence with the scanning laser ophthalmoscope. *Invest Ophthalmol Vis Sci*. 2011;52:9379–9390.
2. Birnbach CD, Jarvelainen M, Possin DE, Milam AH. Histopathology and immunocytochemistry of the neurosensory retina in fundus flavimaculatus. *Ophthalmology*. 1994;101:1211–1219.
3. Sparrow JR, Nakanishi K, Parish CA. The lipofuscin fluorophore A2E mediates blue light-induced damage to retinal pigmented epithelial cells. *Invest Ophthalmol Vis Sci*. 2000;41:1981–1989.
4. Sparrow JR, Duncker T. Fundus Autofluorescence and RPE lipofuscin in age-related macular degeneration. *J Clin Med*. 2014;3:1302–1321.
5. Gliem M, Müller PL, Finger RP, McGuinness MB, Holz FG, Charbel Issa P. Quantitative fundus autofluorescence in early and intermediate age-related macular degeneration. *JAMA Ophthalmol*. 2016;134:817–824.
6. Booij JC, Baas DC, Beisekeeva J, Gorgels TG, Bergen AA. The dynamic nature of Bruch's membrane. *Prog Retin Eye Res*. 2010;29:1–18.
7. Charbel Issa P, Finger RP, Götting C, Hendig D, Holz FG, Scholl HP. Centrifugal fundus abnormalities in pseudoxanthoma elasticum. *Ophthalmology*. 2010;117:1406–1414.
8. Gliem M, Zaeytijd JD, Finger RP, Holz FG, Leroy BP, Charbel Issa P. An update on the ocular phenotype in patients with pseudoxanthoma elasticum. *Front Genet*. 2013;4:14.
9. Gliem M, Hendig D, Finger RP, Holz FG, Charbel Issa P. Reticular pseudodrusen associated with a diseased Bruch membrane in pseudoxanthoma elasticum. *JAMA Ophthalmol*. 2015;133:581–588.
10. Gliem M, Müller PL, Birtel J, Hendig D, Holz FG, Charbel Issa P. Frequency, phenotypic characteristics and progression of atrophy associated with a diseased Bruch's Membrane in pseudoxanthoma elasticum. *Invest Ophthalmol Vis Sci*. 2016;57:3323–3330.
11. Schulz V, Hendig D, Henjakovic M, Szliska C, Kleesiek K, Götting C. Mutational analysis of the ABCC6 gene and the proximal ABCC6 gene promoter in German patients with pseudoxanthoma elasticum (PXE). *Hum Mutat*. 2006;27:831.
12. Costrop LM, Vanakker OO, Van Laer L, et al. Novel deletions causing pseudoxanthoma elasticum underscore the genomic instability of the ABCC6 region. *J Hum Genet*. 2010;55:112–117.
13. Plomp AS, Toonstra J, Bergen AA, van Dijk MR, de Jong PT. Proposal for updating the pseudoxanthoma elasticum classification system and a review of the clinical findings. *Am J Med Genet A*. 2010;152A:1049–1058.
14. Müller PL, Gliem M, Mangold E, et al. Monoallelic ABCA4 mutations appear insufficient to cause retinopathy: a quantitative autofluorescence study. *Invest Ophthalmol Vis Sci*. 2015;56:8179–8186.
15. Charbel Issa P, Finger RP, Holz FG, Scholl HP. Multimodal imaging including spectral domain OCT and confocal near infrared reflectance for characterization of outer retinal pathology in pseudoxanthoma elasticum. *Invest Ophthalmol Vis Sci*. 2009;50:5913–5918.
16. Duncker T, Tsang SH, Woods RL, et al. Quantitative fundus autofluorescence and optical coherence tomography in PRPH2/RDS- and ABCA4-associated disease exhibiting phenotypic overlap. *Invest Ophthalmol Vis Sci*. 2015;56:3159–3170.
17. Jacobson SG, Cideciyan AV, Bennett J, Kingsley RM, Sheffield VC, Stone EM. Novel mutation in the TIMP3 gene causes Sorsby fundus dystrophy. *Arch Ophthalmol*. 2002;120:376–379.
18. Jacobson SG, Cideciyan AV, Wright E, Wright AF. Phenotypic marker for early disease detection in dominant late-onset retinal degeneration. *Invest Ophthalmol Vis Sci*. 2001;42:1882–1890.
19. Gliem M, Müller PL, Mangold E, et al. Sorsby fundus dystrophy: novel mutations, novel phenotypic characteristics, and treatment outcomes. *Invest Ophthalmol Vis Sci*. 2015;56:2664–2676.
20. Burke TR, Duncker T, Woods RL, et al. Quantitative fundus autofluorescence in recessive Stargardt disease. *Invest Ophthalmol Vis Sci*. 2014;55:2841–2852.
21. Jager RD, Mieler WF, Miller JW. Age-related macular degeneration. *N Engl J Med*. 2008;358:2606–2617.
22. Swaroop A, Chew EY, Rickman CB, Abecasis GR. Unraveling a multifactorial late-onset disease: from genetic susceptibility to disease mechanisms for age-related macular degeneration. *Annu Rev Genomics Hum Genet*. 2009;10:19–43.
23. Ramrattan RS, van der Schaft TL, Mooy CM, de Bruijn WC, Mulder PG, de Jong PT. Morphometric analysis of Bruch's membrane, the choriocapillaris, and the choroid in aging. *Invest Ophthalmol Vis Sci*. 1994;35:2857–2864.
24. Spraul CW, Lang GE, Grossniklaus HE, Lang GK. Histologic and morphometric analysis of the choroid, Bruch's membrane, and retinal pigment epithelium in postmortem eyes with age-related macular degeneration and histologic examination of surgically excised choroidal neovascular membranes. *Surv Ophthalmol*. 1999;44(suppl 1):S10–S32.
25. Glenn JV, Mahaffy H, Wu K, et al. Advanced glycation end product (AGE) accumulation on Bruch's membrane: links to age-related RPE dysfunction. *Invest Ophthalmol Vis Sci*. 2009;50:441–451.
26. Curcio CA, Johnson M, Rudolf M, Huang JD. The oil spill in ageing Bruch membrane. *Br J Ophthalmol*. 2011;95:1638–1645.

Investigative Ophthalmology & Visual Science

27. Pauleikhoff D, Harper CA, Marshall J, Bird AC. Aging changes in Bruch's membrane. A histochemical and morphologic study. *Ophthalmology.* 1990;97:171–178.

28. Flamendorf J, Agron E, Wong WT, et al. Impairments in Dark adaptation are associated with age-related macular degeneration severity and reticular pseudodrusen. *Ophthalmology.* 2015;122:2053–2062.

29. Owsley C, McGwin G Jr, Clark ME, et al. Delayed rod-mediated dark adaptation is a functional biomarker for incident early age-related macular degeneration. *Ophthalmology.* 2016;123:344–351.

Investigative Ophthalmology & Visual Science